DESY 02-079
June 2002
ISSN 0418-9833

Measurement of Inclusive Jet Cross-Sections in Deep-Inelastic *ep* Scattering at HERA

H1 Collaboration

Abstract

A measurement of inclusive jet cross-sections in deep-inelastic ep scattering at HERA is presented based on data with an integrated luminosity of $21.1\ \mathrm{pb}^{-1}$. The measurement is performed for photon virtualities Q^2 between 5 and $100\ \mathrm{GeV}^2$, differentially in Q^2, in the jet transverse energy E_T, in E_T^2/Q^2 and in the pseudorapidity η_{lab}. With the renormalization scale $\mu_R = E_T$, perturbative QCD calculations in next-to-leading order (NLO) give a good description of the data in most of the phase space. Significant discrepancies are observed only for jets in the proton beam direction with E_T below 20 GeV and Q^2 below $20\ \mathrm{GeV}^2$. This corresponds to the region in which NLO corrections are largest and further improvement of the calculations is thus of particular interest.

To be submitted to Phys. Lett.

C. Adloff[33], V. Andreev[24], B. Andrieu[27], T. Anthonis[4], A. Astvatsatourov[35], A. Babaev[23], J. Bähr[35], P. Baranov[24], E. Barrelet[28], W. Bartel[10], S. Baumgartner[36], J. Becker[37], M. Beckingham[21], A. Beglarian[34], O. Behnke[13], C. Beier[14], A. Belousov[24], Ch. Berger[1], T. Berndt[14], J.C. Bizot[26], J. Böhme[10], V. Boudry[27], W. Braunschweig[1], V. Brisson[26], H.-B. Bröker[2], D.P. Brown[10], W. Brückner[12], D. Bruncko[16], F.W. Büsser[11], A. Bunyatyan[12,34], A. Burrage[18], G. Buschhorn[25], L. Bystritskaya[23], A.J. Campbell[10], T. Carli[10,25], S. Caron[1], F. Cassol-Brunner[22], D. Clarke[5], C. Collard[4], J.G. Contreras[7,41], Y.R. Coppens[3], J.A. Coughlan[5], M.-C. Cousinou[22], B.E. Cox[21], G. Cozzika[9], J. Cvach[29], J.B. Dainton[18], W.D. Dau[15], K. Daum[33,39], M. Davidsson[20], B. Delcourt[26], N. Delerue[22], R. Demirchyan[34], A. De Roeck[10,43], E.A. De Wolf[4], C. Diaconu[22], J. Dingfelder[13], P. Dixon[19], V. Dodonov[12], J.D. Dowell[3], A. Droutskoi[23], A. Dubak[25], C. Duprel[2], G. Eckerlin[10], D. Eckstein[35], V. Efremenko[23], S. Egli[32], R. Eichler[36], F. Eisele[13], E. Eisenhandler[19], M. Ellerbrock[13], E. Elsen[10], M. Erdmann[10,40,e], W. Erdmann[36], P.J.W. Faulkner[3], L. Favart[4], A. Fedotov[23], R. Felst[10], J. Ferencei[10], S. Ferron[27], M. Fleischer[10], P. Fleischmann[10], Y.H. Fleming[3], G. Flügge[2], A. Fomenko[24], I. Foresti[37], J. Formánek[30], G. Franke[10], G. Frising[1], E. Gabathuler[18], K. Gabathuler[32], J. Garvey[3], J. Gassner[32], J. Gayler[10], R. Gerhards[10], C. Gerlich[13], S. Ghazaryan[4,34], L. Goerlich[6], N. Gogitidze[24], C. Grab[36], V. Grabski[34], H. Grässler[2], T. Greenshaw[18], G. Grindhammer[25], T. Hadig[13], D. Haidt[10], L. Hajduk[6], J. Haller[13], W.J. Haynes[5], B. Heinemann[18], G. Heinzelmann[11], R.C.W. Henderson[17], S. Hengstmann[37], H. Henschel[35], R. Heremans[4], G. Herrera[7,44], I. Herynek[29], M. Hildebrandt[37], M. Hilgers[36], K.H. Hiller[35], J. Hladký[29], P. Höting[2], D. Hoffmann[22], R. Horisberger[32], A. Hovhannisyan[34], S. Hurling[10], M. Ibbotson[21], Ç. İşsever[7], M. Jacquet[26], M. Jaffre[26], L. Janauschek[25], X. Janssen[4], V. Jemanov[11], L. Jönsson[20], C. Johnson[3], D.P. Johnson[4], M.A.S. Jones[18], H. Jung[20,10], D. Kant[19], M. Kapichine[8], M. Karlsson[20], O. Karschnick[11], F. Keil[14], N. Keller[37], J. Kennedy[18], I.R. Kenyon[3], S. Kermiche[22], C. Kiesling[25], P. Kjellberg[20], M. Klein[35], C. Kleinwort[10], T. Kluge[1], G. Knies[10], B. Koblitz[25], S.D. Kolya[21], V. Korbel[10], P. Kostka[35], S.K. Kotelnikov[24], R. Koutouev[12], A. Koutov[8], J. Kroseberg[37], K. Krüger[10], T. Kuhr[11], T. Kurča[16], D. Lamb[3], M.P.J. Landon[19], W. Lange[35], T. Laštovička[35,30], P. Laycock[18], E. Lebailly[26], A. Lebedev[24], B. Leißner[1], R. Lemrani[10], V. Lendermann[7], S. Levonian[10], M. Lindstroem[20], B. List[36], E. Lobodzinska[10,6], B. Lobodzinski[6,10], A. Loginov[23], N. Loktionova[24], V. Lubimov[23], S. Lüders[36], D. Lüke[7,10], L. Lytkin[12], N. Malden[21], E. Malinovski[24], I. Malinovski[24], S. Mangano[36], R. Maraček[25], P. Marage[4], J. Marks[13], R. Marshall[21], H.-U. Martyn[1], J. Martyniak[6], S.J. Maxfield[18], D. Meer[36], A. Mehta[18], K. Meier[14], A.B. Meyer[11], H. Meyer[33], J. Meyer[10], P.-O. Meyer[2], S. Mikocki[6], D. Milstead[18], S. Mohrdieck[11], M.N. Mondragon[7], F. Moreau[27], A. Morozov[8], J.V. Morris[5], K. Müller[37], P. Murín[16,42], V. Nagovizin[23], B. Naroska[11], J. Naumann[7], Th. Naumann[35], G. Nellen[25], P.R. Newman[3], F. Niebergall[11], C. Niebuhr[10], O. Nix[14], G. Nowak[6], J.E. Olsson[10], D. Ozerov[23], V. Panassik[8], C. Pascaud[26], G.D. Patel[18], M. Peez[22], E. Perez[9], A. Petrukhin[35], J.P. Phillips[18], D. Pitzl[10], R. Pöschl[26], I. Potachnikova[12], B. Povh[12], G. Rädel[1], J. Rauschenberger[11], P. Reimer[29], B. Reisert[25], C. Risler[25], E. Rizvi[3], P. Robmann[37], R. Roosen[4], A. Rostovtsev[23], S. Rusakov[24], K. Rybicki[6], J. Samson[36], D.P.C. Sankey[5], S. Schätzel[13], J. Scheins[1], F.-P. Schilling[10], P. Schleper[10], D. Schmidt[33], D. Schmidt[10], S. Schmidt[25], S. Schmitt[10], M. Schneider[22], L. Schoeffel[9], A. Schöning[36], T. Schörner-Sadenius[25], V. Schröder[10], H.-C. Schultz-Coulon[7], C. Schwanenberger[10], K. Sedlák[29], F. Sefkow[37], V. Shekelyan[25], I. Sheviakov[24], L.N. Shtarkov[24], Y. Sirois[27], T. Sloan[17], P. Smirnov[24], Y. Soloviev[24], D. South[21], V. Spaskov[8], A. Specka[27], H. Spitzer[11],

R. Stamen[7], B. Stella[31], J. Stiewe[14], I. Strauch[10], U. Straumann[37], M. Swart[14], S. Tchetchelnitski[23], G. Thompson[19], P.D. Thompson[3], F. Tomasz[14], D. Traynor[19], P. Truöl[37], G. Tsipolitis[10,38], I. Tsurin[35], J. Turnau[6], J.E. Turney[19], E. Tzamariudaki[25], S. Udluft[25], A. Uraev[23], M. Urban[37], A. Usik[24], S. Valkár[30], A. Valkárová[30], C. Vallée[22], P. Van Mechelen[4], S. Vassiliev[8], Y. Vazdik[24], A. Vest[1], A. Vichnevski[8], K. Wacker[7], J. Wagner[10], R. Wallny[37], B. Waugh[21], G. Weber[11], D. Wegener[7], C. Werner[13], N. Werner[37], M. Wessels[1], G. White[17], S. Wiesand[33], T. Wilksen[10], M. Winde[35], G.-G. Winter[10], Ch. Wissing[7], M. Wobisch[10], E.-E. Woehrling[3], E. Wünsch[10], A.C. Wyatt[21], J. Žáček[30], J. Zálešák[30], Z. Zhang[26], A. Zhokin[23], F. Zomer[26], and M. zur Nedden[10]

[1] *I. Physikalisches Institut der RWTH, Aachen, Germany*[a]
[2] *III. Physikalisches Institut der RWTH, Aachen, Germany*[a]
[3] *School of Physics and Space Research, University of Birmingham, Birmingham, UK*[b]
[4] *Inter-University Institute for High Energies ULB-VUB, Brussels; Universiteit Antwerpen (UIA), Antwerpen; Belgium*[c]
[5] *Rutherford Appleton Laboratory, Chilton, Didcot, UK*[b]
[6] *Institute for Nuclear Physics, Cracow, Poland*[d]
[7] *Institut für Physik, Universität Dortmund, Dortmund, Germany*[a]
[8] *Joint Institute for Nuclear Research, Dubna, Russia*
[9] *CEA, DSM/DAPNIA, CE-Saclay, Gif-sur-Yvette, France*
[10] *DESY, Hamburg, Germany*
[11] *Institut für Experimentalphysik, Universität Hamburg, Hamburg, Germany*[a]
[12] *Max-Planck-Institut für Kernphysik, Heidelberg, Germany*
[13] *Physikalisches Institut, Universität Heidelberg, Heidelberg, Germany*[a]
[14] *Kirchhoff-Institut für Physik, Universität Heidelberg, Heidelberg, Germany*[a]
[15] *Institut für experimentelle und Angewandte Physik, Universität Kiel, Kiel, Germany*
[16] *Institute of Experimental Physics, Slovak Academy of Sciences, Košice, Slovak Republic*[e,f]
[17] *School of Physics and Chemistry, University of Lancaster, Lancaster, UK*[b]
[18] *Department of Physics, University of Liverpool, Liverpool, UK*[b]
[19] *Queen Mary and Westfield College, London, UK*[b]
[20] *Physics Department, University of Lund, Lund, Sweden*[g]
[21] *Physics Department, University of Manchester, Manchester, UK*[b]
[22] *CPPM, CNRS/IN2P3 - Univ Mediterranee, Marseille - France*
[23] *Institute for Theoretical and Experimental Physics, Moscow, Russia*[l]
[24] *Lebedev Physical Institute, Moscow, Russia*[e]
[25] *Max-Planck-Institut für Physik, München, Germany*
[26] *LAL, Université de Paris-Sud, IN2P3-CNRS, Orsay, France*
[27] *LPNHE, Ecole Polytechnique, IN2P3-CNRS, Palaiseau, France*
[28] *LPNHE, Universités Paris VI and VII, IN2P3-CNRS, Paris, France*
[29] *Institute of Physics, Academy of Sciences of the Czech Republic, Praha, Czech Republic*[e,i]
[30] *Faculty of Mathematics and Physics, Charles University, Praha, Czech Republic*[e,i]
[31] *Dipartimento di Fisica Università di Roma Tre and INFN Roma 3, Roma, Italy*
[32] *Paul Scherrer Institut, Villigen, Switzerland*
[33] *Fachbereich Physik, Bergische Universität Gesamthochschule Wuppertal, Wuppertal, Germany*
[34] *Yerevan Physics Institute, Yerevan, Armenia*

[35] *DESY, Zeuthen, Germany*
[36] *Institut für Teilchenphysik, ETH, Zürich, Switzerland*[j]
[37] *Physik-Institut der Universität Zürich, Zürich, Switzerland*[j]

[38] *Also at Physics Department, National Technical University, Zografou Campus, GR-15773 Athens, Greece*
[39] *Also at Rechenzentrum, Bergische Universität Gesamthochschule Wuppertal, Germany*
[40] *Also at Institut für Experimentelle Kernphysik, Universität Karlsruhe, Karlsruhe, Germany*
[41] *Also at Dept. Fis. Ap. CINVESTAV, Mérida, Yucatán, México*[k]
[42] *Also at University of P.J. Šafárik, Košice, Slovak Republic*
[43] *Also at CERN, Geneva, Switzerland*
[44] *Also at Dept. Fis. CINVESTAV, México City, México*[k]

[a] *Supported by the Bundesministerium für Bildung und Forschung, FRG, under contract numbers 05 H1 1GUA /1, 05 H1 1PAA /1, 05 H1 1PAB /9, 05 H1 1PEA /6, 05 H1 1VHA /7 and 05 H1 1VHB /5*
[b] *Supported by the UK Particle Physics and Astronomy Research Council, and formerly by the UK Science and Engineering Research Council*
[c] *Supported by FNRS-FWO-Vlaanderen, IISN-IIKW and IWT*
[d] *Partially Supported by the Polish State Committee for Scientific Research, grant no. 2P0310318 and SPUB/DESY/P03/DZ-1/99 and by the German Bundesministerium für Bildung und Forschung*
[e] *Supported by the Deutsche Forschungsgemeinschaft*
[f] *Supported by VEGA SR grant no. 2/1169/2001*
[g] *Supported by the Swedish Natural Science Research Council*
[i] *Supported by the Ministry of Education of the Czech Republic under the projects INGO-LA116/2000 and LN00A006, by GAUK grant no 173/2000*
[j] *Supported by the Swiss National Science Foundation*
[k] *Supported by CONACyT*
[l] *Partially Supported by Russian Foundation for Basic Research, grant no. 00-15-96584*

1 Introduction

HERA offers excellent possibilities to test predictions of quantum chromodynamics (QCD), the theory of the strong interaction, in deep-inelastic electron[1] proton scattering (DIS). This theory has been successfully tested to a very high level of precision in the measurements of the proton structure function F_2 [1, 2], in which the photon virtuality Q^2 gives rise to a hard scale. QCD also predicts the production of partons with large transverse momenta, which fragment into hadronic jets with similar four-momenta. Jet observables therefore give direct access to the underlying parton dynamics. In addition to $\sqrt{Q^2}$, the transverse energies E_T of the resulting jets, measured in an appropriate frame of reference, provide a natural hard scale for the description of the interaction within perturbative QCD.

Jets have been studied extensively at HERA and at other colliders. Recent measurements of (multi-)jet cross-sections at HERA [3–6] have shown that at sufficiently large values of the photon virtuality $Q^2 \gtrsim 150\ \mathrm{GeV}^2$, calculations implementing matrix elements to $\mathcal{O}(\alpha_s^2)$ in the strong coupling constant, i.e. next-to-leading order (NLO), are in excellent agreement with the data. These highly successful calculations are performed in the conventional collinear approximation referred to as DGLAP [7]. Since in this kinematic regime of large Q^2, the theoretical uncertainties are small, the measured cross-sections have been used to extract α_s [3, 6] and the gluon density of the proton [3]. For some observables these data can be described even at lower values of Q^2, although the theoretical uncertainties in the predictions and the QCD corrections between leading order (LO) and NLO predictions increase in this kinematic region.

Problems have also been encountered in the theoretical description of jets in DIS. Measurements of highly energetic jets at large pseudorapidities[2] η_{lab} with transverse energies squared of the order of Q^2 (so-called forward jets [8]) made by the H1 [9] and ZEUS [10, 11] collaborations show large discrepancies between data and NLO calculations at low values of Bjorken-x. This may be due to a breakdown of the DGLAP approximation and the onset of BFKL [12] effects where, in contrast to DGLAP, the emissions of partons are not ordered in transverse momentum. Alternatively, a good description of the data can be obtained [13] by considering the partonic structure of the virtual photon, which is expected to be important for $E_T^2 > Q^2$ and Q^2 not too large. It has been pointed out [14], however, that there is some correspondence between higher order effects and resolved virtual photon contributions. Further discrepancies between NLO calculations and data were revealed by H1 measurements of DIS dijet production for $Q^2 < 11\ \mathrm{GeV}^2$ [15] and for $Q^2 < 10\ \mathrm{GeV}^2$ with invariant dijet masses $M_{jj} < 25\ \mathrm{GeV}$ or mean dijet $E_T < 20\ \mathrm{GeV}$ [3]. In these regions of phase space the NLO corrections to the LO cross-sections are large, such that next-to-next-to-leading order (NNLO) contributions are also likely to be important.

While the H1 measurements of dijet [3] and three-jet production [4] mentioned above cover low and high Q^2 values, inclusive jet production in DIS has only been measured previously at high values of Q^2 above 150 GeV^2 [3]. This paper presents precision measurements of inclusive

[1] In the following, the generic name "electron" will be used for the beam and scattered lepton.

[2] The pseudorapidity η_{lab} is defined as $\eta_{\mathrm{lab}} = -\ln\tan(\theta/2)$, with the polar angle θ being measured with respect to the positive z-axis, which is given by the proton beam (or forward) direction.

jet cross-sections in the Breit frame[3] at low Q^2 values ($5 < Q^2 < 100\,\mathrm{GeV}^2$). Here, "inclusive" means that in every selected event every jet that passes the experimental cuts contributes to the measured cross-section. The advantages of investigating QCD with studies of inclusive jets compared with multi-jets are two-fold. First, the accessible phase space is extended. Second, phase space regions in which fixed order calculations are infrared-sensitive are naturally avoided. In dijet analyses such regions are usually suppressed by imposing asymmetric cuts on the transverse jet energies [16].

2 Experimental apparatus

A detailed description of the H1 apparatus can be found elsewhere [17, 18]. Here, only the components of the detector which are relevant for the measurement of low Q^2 jet cross-sections are introduced.

The scattered electron is measured with a calorimeter made of lead and scintillating fibres (SpaCal) [19]. The SpaCal covers polar angles from 153° to 177.5° for collisions at the nominal interaction point. It is divided into an electromagnetic section with 28 radiation lengths and a hadronic section and has a total depth of 2 interaction lengths. The electromagnetic section of the SpaCal has an energy resolution of $\sigma_E/E \approx 0.07/\sqrt{E[\mathrm{GeV}]} \oplus 0.01$ for electrons [20]. In addition, a backward planar drift chamber in front of the SpaCal with an angular acceptance of $151^\circ < \theta < 177.5^\circ$ serves to suppress photoproduction background, where a high energy hadron fakes an electron.

The hadronic final state is measured using the SpaCal and the liquid argon (LAr) calorimeter [21] together with the tracking chambers. The LAr calorimeter provides full azimuthal coverage over the polar angle range $4^\circ < \theta < 154^\circ$ with a depth ranging between 4.5 and 8 interaction lengths, depending on the polar angle. Test beam measurements of the LAr calorimeter modules showed an energy resolution of $\sigma_E/E \approx 0.50/\sqrt{E[\mathrm{GeV}]} \oplus 0.02$ for charged pions after software energy reweighting [22] and of $\sigma_E/E \approx 0.12/\sqrt{E[\mathrm{GeV}]} \oplus 0.01$ for electrons [23].

The calorimeters are surrounded by a superconducting solenoid which provides a uniform magnetic field of 1.15 T parallel to the beam axis in the region of the central tracking detectors. Charged particles are measured in this central tracking area which consists of drift and proportional chambers. The drift chambers cover a range in polar angle from 15° to 165°. The tracking chambers also serve for the determination of the event vertex.

3 QCD calculations and Monte Carlo models

For the NLO calculation of jet observables at the parton level the DISENT computer program [24] was used. Several other programs [25–27] are known to give comparable results [28]. All of these programs calculate the direct photon induced contributions to the cross-section.

[3]The Breit frame is defined by $2x\vec{p} + \vec{q} = 0$, where x is the Bjorken scaling variable, and $\vec{p}$ and $\vec{q}$ are the proton and the virtual photon momenta, respectively.

Only the JetViP program [25] provides the additional possibility to calculate a cross-section consisting of both direct and resolved photon contributions. While implementing the concept of the resolved hadronic substructure of the photon is straightforward for photoproduction, in the DIS case conceptual difficulties are encountered [29] which lead to ambiguous results. Therefore we decided not to use JetViP for comparisons with the present data.

In the DISENT program the square of the renormalization scale, μ_R^2, can be set to any linear combination of the two hard scales in the event, E_T^2 and Q^2. Here, E_T is the transverse energy of the jet in the Breit frame in the case of events in which only one jet satisfies the selection criteria. In the case of two or more selected jets, E_T was set to the mean transverse energy of the two hardest jets. For most of the comparisons with data $\mu_R = E_T$ was chosen, since $E_T^2 > Q^2$ in almost all of the phase space considered. However, the effects of choosing $\mu_R = \sqrt{Q^2}$ are also discussed in section 5. The factorization scale was always set to $\sqrt{Q^2}$. In the kinematic region considered in this analysis the cross-section predictions are stable within a few percent even for large variations of the factorization scale [30]. The parton density functions (PDF) of the proton were taken from the CTEQ5M (CTEQ5L) parameterization [31] for the calculation of the NLO (LO) cross-sections. For NLO, the corresponding value of $\alpha_s(M_Z)$ is 0.118. The number of active flavours was chosen to be $n_f = 5$ unless μ_R^2 was less than 25 GeV^2 in which case $n_f = 4$ was used in order to simulate the threshold for the onset of beauty production via the boson gluon fusion process.

In contrast to fixed order QCD calculations, which can only predict the partonic final state of an event, the implementation of phenomenological QCD models in Monte Carlo (MC) generators allows the details of the hadronic final state to be simulated. These generators typically implement $\mathcal{O}(\alpha_s)$ matrix elements and account for the effects of higher orders using different QCD-inspired mechanisms. LEPTO [32] and RAPGAP [33] are so-called ME+PS Monte Carlo programs which combine the $\mathcal{O}(\alpha_s)$ matrix elements with parton showers which take into account the leading logarithms in Q^2 to all orders. As an alternative approach, the ARIADNE MC [34] simulates parton cascades as a chain of independently radiating colour dipoles according to [35]. Higher order QED corrections, which can influence the event topology and the size of the cross-sections, are implemented in the program HERACLES [36] which is interfaced to RAPGAP. An interface to LEPTO and ARIADNE is provided by the DJANGO [37] program. In the present analysis the MC generators ARIADNE and LEPTO were used to estimate the hadronization corrections which were applied to the NLO QCD calculations. RAPGAP and the DJANGO-interfaced ARIADNE program ('DJANGO/ARIADNE') were used to correct the data for detector and higher order QED effects (see section 4.2). For all MC generators used in the analysis, the hadronization of the final partonic system as well as the particle decays were modelled with the Lund colour string model [38] as implemented in JETSET [39].

4 Measurement

4.1 Event and jet selection

The analysed data were collected with the H1 detector in the years 1996 and 1997. In this running period HERA collided 27.5 GeV positrons with 820 GeV protons. The integrated luminosity as measured using the bremsstrahlung process $ep \to ep\gamma$ amounts to 21.1 pb^{-1}.

The events are triggered by demanding a localized energy deposition in the SpaCal and loose track requirements. The trigger efficiencies are close to 100 $\%$. DIS events are selected by identifying the scattered electron in the SpaCal. More precisely, the electron is defined as the highest energy cluster in the SpaCal with an energy of at least 10 GeV. It must be detected at a polar angle $\theta > 156^\circ$ to guarantee the full reconstruction of the particle within the SpaCal acceptance.

The kinematic variables x, Q^2 and y are determined using electron information only, according to $Q^2 = 4E_eE'_e\cos^2(\theta_e/2)$, $y = 1 - (E'_e/E_e)\sin^2(\theta_e/2)$ and $x = Q^2/(ys)$, where E_e, E'_e and θ_e are the electron beam energy, the energy of the scattered electron and the electron scattering angle, respectively. The latter two quantities are measured using the SpaCal. The center-of-mass energy squared s of the proton-electron scattering is computed from the beam energies.

The kinematic range considered in this analysis is further constrained by the conditions $5 < Q^2 < 100\,\mathrm{GeV}^2$ and $0.2 < y < 0.6$. The latter condition also leads to a reduction of photoproduction background and of events in which the incoming electron radiates a high-energy photon.

The hadronic final state objects of an event are reconstructed using information from energy deposits in the calorimeters and from tracks in the inner detectors. A cut $\sum_j(E_j - P_{z,j}) > 45\,\mathrm{GeV}$ further suppresses radiative events. Here the sum runs over the objects of the hadronic final state and the scattered lepton. An additional cut $\sum_j(E_j - P_{z,j}) < 65\,\mathrm{GeV}$ reduces non-ep background. For all events the reconstructed z-coordinate of the event vertex is required to be within $\pm 35\,\mathrm{cm}$ of its nominal position which further reduces non-ep background to a negligible level.

Jets are defined using the inclusive $k_\perp$ cluster algorithm [40] in the Breit frame in which the photon and the parton collide head-on. This ensures that the jet transverse energies are closely related to those of the partons emerging from the hard scattering. Jets are finally selected by requiring their transverse energy to be larger than 5 GeV. In addition, the jets have to be well contained within the polar angle acceptance of the LAr calorimeter. Therefore, a cut on the pseudorapidity of the jets $-1 < \eta_{\mathrm{lab}} < 2.8$ is applied.

4.2 Correction procedure

All data distributions shown in this paper are corrected for the effects of limited detector acceptance and resolution and for higher-order QED effects using a bin-to-bin correction method. Following studies of migrations made with simulated events, the bin sizes were chosen in order to ensure that this method can be applied. In all bins, the stability[4] and purity exceed 40$\%$. The distributions of kinematic variables and jet observables in the data are sufficiently well described by the QCD Monte Carlo models used in the correction procedure. RAPGAP describes the data very well for transverse energies above 10 GeV but lies below the data for $E_T < 10$ GeV. The DJANGO/ARIADNE program gives a good description for $E_T < 10$ GeV, but is too high for higher values of the transverse energy.

[4]The stability (purity) is defined as the number of jets which are both generated and reconstructed in an analysis bin, divided by the total number of jets that are generated (reconstructed) in that bin.

The correction factor is defined as the ratio of the number of events from two different MC event samples generated for the same phase space. The first sample has no QED corrections and is not subjected to the detector simulation. The second sample includes QED corrections to the leptonic vertex of the interaction and is subjected to a full simulation of the H1 detector and reconstruction procedure. The correction factors were calculated from both the RAPGAP and the DJANGO/ARIADNE programs. The final correction was taken to be the average of the two results. The corrections factors thus derived are typically between 0.9 and 1.1. Values down to 0.7 and up to 1.3 are reached in some exceptional analysis bins, for example for $E_T^2/Q^2 < 2$ and $E_T^2/Q^2 > 50$ for jets in the forward region $1.5 < \eta_{\rm lab} < 2.8$. Although the shapes and normalizations of the predicted cross-sections differ significantly between RAGPAP and DJANGO/ARIADNE, the difference between the correction factors derived with the two programs is usually as small as 5 to 10$\%$. Half of this difference is assigned as the systematic error in the correction procedure.

In order to compare the data, which are corrected for instrumental and radiative effects, to the NLO QCD calculations, hadronization corrections are applied to the latter. They were estimated using the predictions of the Monte Carlo programs LEPTO and ARIADNE for the ratio of the hadron level to the parton level cross-sections. The average of the two predictions is taken as the correction. The effects of hadronization reduce the NLO cross-sections by factors that vary from 0.85 to 0.95 with increasing jet transverse energy or Q^2 [41]. The uncertainty in the hadronization correction is taken to be half the difference between the predictions of the two programs.

The treatment of systematic uncertainties is similar to that in [3, 4]. The dominant contribution to the total systematic error stems from the uncertainty in the hadronic energy scale of the LAr calorimeter, which is taken to be 3% for this analysis. This uncertainty leads to an uncertainty in the measured cross-sections of 10 to 15$\%$. All other sources of systematic uncertainties, such as the method used for the reconstruction of kinematic variables, the determination of the energy and polar angle of the scattered electron and the model dependence of the correction procedure, are small by comparison.

5 Results

In this section the results of the inclusive jet measurement described in section 4 are compared with LO and NLO QCD calculations as explained in section 3. The data are presented in figures 1 to 4. In the top parts of the figures, the data, corrected for detector and radiative effects, are compared with the results of the LO and NLO QCD calculations without hadronization corrections. The uncertainty in the NLO predictions, which was estimated by varying the renormalization scale μ_R by a factor of ± 2, is also shown. In the bottom part of the figures, the consistency of the NLO QCD prediction with the data is studied in more detail by plotting the relative difference (QCD-Data)/Data. Here "QCD" denotes the NLO prediction corrected for hadronization effects as discussed in section 4.2. Both the uncertainty due to the hadronization correction and the effect of the variation of the renormalization scale μ_R are indicated. All measured cross-sections and their errors are given in tables 1, 2 and 3, together with the average Bjorken-x and Q^2 values of the measurements, taken from the data.

Figure 1 shows the inclusive jet cross-section as a function of the transverse jet energy E_T in different regions of the pseudorapidity $\eta_{\rm lab}$: in the backward region $-1 < \eta_{\rm lab} < 0.5$, the central region $0.5 < \eta_{\rm lab} < 1.5$ and the forward (proton direction) region $1.5 < \eta_{\rm lab} < 2.8$. The measured cross-sections, which extend over four orders of magnitude, are compared to the QCD calculations using a renormalization scale $\mu_R = E_T$.

While there is good agreement between the data and the NLO QCD calculation in the backward region for all E_T values, discrepancies are observed for more forward jets with low E_T. At the lowest E_T, $5 < E_T < 20$ GeV, for $\eta_{\rm lab} > 1.5$, the assumed renormalization scale uncertainty does not cover the large difference between data and QCD calculation. Figure 1 shows that the discrepancies are accompanied by large corrections between LO and NLO calculations. The NLO predictions are up to a factor 5 larger than the LO ones. Furthermore, the effects of a variation of the renormalization scale, which are indicated by the hatched band, are largest for these low E_T jets in the forward region.

In figure 2, the jet E_T distribution in the forward region only is presented in five different intervals of Q^2. Whereas for $Q^2 > 20\ \mathrm{GeV}^2$ the data can be described by the NLO predictions even for transverse energies below 20 GeV, for $Q^2 < 20\ \mathrm{GeV}^2$ the NLO calculation falls short of the data by a factor of up to two for $E_T < 20\ \mathrm{GeV}$. As in fig. 1 these discrepancies between data and predictions are accompanied by large NLO/LO corrections.

One can conclude that the perturbative NLO QCD calculations work reasonably well in most of the rapidity range, even in the forward region $\eta_{\rm lab} > 1.5$, as long as both E_T and Q^2 are not too small.

In order to study the interplay of the two possible scales in DIS jet events, figure 3 shows the inclusive jet cross-section as a function of the ratio E_T^2/Q^2 for the different regions of $\eta_{\rm lab}$. The data are well described by the NLO calculations over the full E_T^2/Q^2 range only in the backward region $-1 < \eta_{\rm lab} < 0.5$. For the central and even more for the forward pseudorapidities, there is a discrepancy between data and calculation for the medium range of this ratio, i.e. $2 < E_T^2/Q^2 < 50$. This region is dominated by small values of E_T^2 and Q^2. For large and small values of E_T^2/Q^2, which are correlated with large values of either E_T^2 or Q^2, the NLO calculation is in agreement with the data. As in the case of $\mathrm{d}\sigma_{\rm Jet}/\mathrm{d}E_T$ the discrepancies occur in regions where the NLO/LO corrections are very large (up to a factor of 6 in the forward region).

Switching to $\mu_R = \sqrt{Q^2}$ (figure 4) changes the situation. In this case, large discrepancies between data and NLO calculation are observed only for large values of $E_T^2/Q^2 > 50$ (and hence low values of Q^2) irrespective of the $\eta_{\rm lab}$ range. This suggests that when Q^2 is much smaller than E_T^2, the variable Q^2 provides too soft a scale and is irrelevant for the description of the hard scattering process. In contrast to the case $\mu_R = E_T$, these discrepancies do not occur in the analysis intervals in which the NLO/LO corrections are largest. Although the data and the predictions are compatible at lower values of E_T^2/Q^2, it should be noted that the choice of $\mu_R = \sqrt{Q^2}$ leads to much larger scale uncertainties than is the case with $\mu_R = E_T$.

6 Summary

Inclusive jet cross-sections have been measured for values of Q^2 between 5 and 100 GeV^2 with the H1 detector at HERA. Jets were selected using the inclusive $k_\perp$ algorithm in the Breit frame

and were required to have a minimum transverse energy of 5 GeV. QCD calculations up to second order of the strong coupling constant α_s, with E_T or $\sqrt{Q^2}$ as renormalization scale, were tested against the data.

With E_T as renormalization scale, the data on $\mathrm{d}\sigma_{\mathrm{Jet}}/\mathrm{d}E_T$ are well described by the NLO QCD calculations for jets of all transverse energies in the backward region and in all η_{lab} regions for high transverse jet energies $E_T > 20\,\mathrm{GeV}$, even though the NLO cross-sections can be more than 3 times larger than the LO cross-sections. The only region in which the NLO QCD predictions fail to describe the data is in the forward region when both the transverse jet energy and Q^2 are relatively small. In this region, discrepancies of up to a factor of two are observed, not considering the scale uncertainties. The regions in which the data cannot be described by the QCD calculations are characterized by large NLO/LO corrections and by a strong dependence on the renormalization scale. It is worth noting that the theoretical uncertainties, which are dominated by the effects of a variation of the renormalization scale, are usually much larger than the experimental errors.

Similarly, the distributions of E_T^2/Q^2 are described by the QCD calculations using $\mu_R = E_T$ everywhere except for the range $2 < E_T^2/Q^2 < 50$ for jets in the forward and central regions. Again, the discrepancies between data and calculation are accompanied by large NLO/LO corrections. For the choice $\mu_R = \sqrt{Q^2}$ the agreement between data and predictions is in general good. However, a very strong dependence of the QCD calculations on the renormalization scale is found which questions whether they can be considered as predictive. For $\mu_R = \sqrt{Q^2}$ and $E_T^2/Q^2 > 50$ the calculations fail to describe the data for all jet pseudorapidities, showing that Q^2 is not an appropriate scale choice if $Q^2 \ll E_T^2$.

The correlation of large NLO/LO corrections and high sensitivity to renormalization scale variations with poor agreement between data and QCD predictions in the case of $\mu_R = E_T$ strongly suggests that the inclusion of higher order (e.g. NNLO) terms in the QCD calculations is necessary in order to describe the data. Since in most analysed intervals the experimental errors are much smaller than the theoretical uncertainties, it is evident that a deeper understanding of low Q^2 DIS jet production will require theoretical progress.

Acknowledgements

We would like to thank M. Seymour for many helpful discussions. We are grateful to the HERA machine group whose outstanding efforts have made and continue to make this experiment possible. We thank the engineers and technicians for their work in constructing and now maintaining the H1 detector, our funding agencies for financial support, the DESY technical staff for continual assistance, and the DESY directorate for the hospitality which they extend to the non DESY members of the collaboration.

References

[1] C. Adloff *et al.* [H1 Collaboration], Eur. Phys. J. C **21** (2001) 33 [hep-ex/0012053].

[2] S. Chekanov *et al.* [ZEUS Collaboration], Eur. Phys. J. C **21** (2001) 443 [hep-ex/0105090].

[3] C. Adloff *et al.* [H1 Collaboration], Eur. Phys. J. C **19** (2001) 289 [hep-ex/0010054].

[4] C. Adloff *et al.* [H1 Collaboration], Phys. Lett. B **515** (2001) 17 [hep-ex/0106078].

[5] S. Chekanov *et al.* [ZEUS Collaboration], Eur. Phys. J. C **23** (2002) 13 [hep-ex/0109029].

[6] J. Breitweg *et al.* [ZEUS Collaboration], Phys. Lett. B **507** (2001) 70 [hep-ex/0102042].

[7] V. N. Gribov and L. N. Lipatov, Yad. Fiz. **15** (1972) 781 and 1218 [Sov. J. Nucl. Phys. **15** (1972) 438 and 675];
Y. L. Dokshitzer, Sov. Phys. JETP **46** (1977) 641 [Zh. Eksp. Teor. Fiz. **73** (1977) 1216];
G. Altarelli and G. Parisi, Nucl. Phys. B **126** (1977) 298.

[8] A. H. Mueller, Nucl. Phys. Proc. Suppl. **18C** (1991) 125, J. Phys. G **G17** (1991) 1443;
J. Kwiecinski, A. D. Martin and P. J. Sutton, Phys. Rev. D **46** (1992) 921;
J. Bartels, A. de Roeck and M. Loewe, Z. Phys. C **54** (1992) 635;
W. Tang, Phys. Lett. B **278** (1992) 363.

[9] C. Adloff *et al.* [H1 Collaboration], Nucl. Phys. B **538** (1999) 3 [hep-ex/9809028].

[10] J. Breitweg *et al.* [ZEUS Collaboration], Eur. Phys. J. C **6** (1999) 239 [hep-ex/9805016].

[11] J. Breitweg *et al.* [ZEUS Collaboration], Phys. Lett. B **474** (2000) 223 [hep-ex/9910043].

[12] E. A. Kuraev, L. N. Lipatov and V. S. Fadin, Sov. Phys. JETP **45** (1977) 199 [Zh. Eksp. Teor. Fiz. **72** (1977) 377];
I. I. Balitsky and L. N. Lipatov, Sov. J. Nucl. Phys. **28** (1978) 822 [Yad. Fiz. **28** (1978) 1597].

[13] H. Jung, L. Jönsson and H. Küster, Eur. Phys. J. C **9** (1999) 383 [hep-ph/9903306].

[14] G. Kramer and B. Pötter, Phys. Lett. B **453** (1999) 295 [hep-ph/9901314].

[15] C. Adloff *et al.* [H1 Collaboration], Eur. Phys. J. C **13** (2000) 415 [hep-ex/9806029].

[16] S. Frixione and G. Ridolfi, Nucl. Phys. B **507** (1997) 315 [hep-ph/9707345];
G. Kramer and B. Pötter, Eur. Phys. J. C **5** (1998) 665 [hep-ph/9804352].

[17] I. Abt *et al.* [H1 Collaboration], Nucl. Instrum. Meth. A **386** (1997) 310.

[18] I. Abt *et al.* [H1 Collaboration], Nucl. Instrum. Meth. A **386** (1997) 348.

[19] R. D. Appuhn *et al.* [H1 SPACAL Group Collaboration], Nucl. Instrum. Meth. A **386** (1997) 397.

[20] T. Nicholls *et al.* [H1 SPACAL Group Collaboration], Nucl. Instrum. Meth. A **374** (1996) 149.

[21] B. Andrieu *et al.* [H1 Calorimeter Group Collaboration], Nucl. Instrum. Meth. A **336** (1993) 460.

[22] B. Andrieu *et al.* [H1 Calorimeter Group Collaboration], Nucl. Instrum. Meth. A **336** (1993) 499.

[23] B. Andrieu *et al.* [H1 Calorimeter Group Collaboration], Nucl. Instrum. Meth. A **350** (1994) 57.

[24] S. Catani and M. H. Seymour, Nucl. Phys. B **485** (1997) 291 [Erratum-ibid. B **510** (1997) 503] [hep-ph/9605323].

[25] B. Pötter, Comput. Phys. Commun. **119** (1999) 45 [hep-ph/9806437];
G. Kramer and B. Pötter, Eur. Phys. J. C **5** (1998) 665 [hep-ph/9804352].

[26] E. Mirkes and D. Zeppenfeld, Phys. Lett. B **380** (1996) 205 [hep-ph/9511448];
E. Mirkes, TTP-97-39 (1997), hep-ph/971224 (1997).

[27] D. Graudenz, hep-ph/9710244.

[28] C. Duprel, T. Hadig, N. Kauer and M. Wobisch, in: *Monte Carlo Generators for HERA Physics* (Hamburg, Germany, 1999), A. Doyle, G. Grindhammer, G. Ingelman, H. Jung, Eds., pp.142, DESY-PROC-1999-02, hep-ph/9910448;
B. Pötter, Comput. Phys. Commun. **133** (2000) 105 [hep-ph/9911221].

[29] B. Pötter, in: *New Trends in HERA Physics* (Schloss Ringberg, Tegernsee, Germany, 2001), G. Grindhammer, B. Kniehl, G. Kramer, W. Ochs, Eds., J. Phys. G **28** (2002) 871 [hep-ph/0110009].

[30] R. Mohr, Dissertation, University of Hamburg (2000), Max-Planck-Institut für Physik, München, MPI-PhE/00-06,
`http://www-h1.desy.de/publications/theses_list.html`.

[31] H. L. Lai *et al.* [CTEQ Collaboration], Eur. Phys. J. C **12** (2000) 375 [hep-ph/9903282].

[32] G. Ingelman, A. Edin and J. Rathsman, Comput. Phys. Commun. **101** (1997) 108 [hep-ph/9605286], `http://www3.tsl.uu.se/thep/lepto/`.

[33] H. Jung, Comput. Phys. Commun. **86** (1995) 147,
`http://www-h1.desy.de/~jung/rapgap.html`.

[34] L. Lönnblad, Comput. Phys. Commun. **71** (1992) 15,
`http://www.thep.lu.se/~leif/ariadne/index.html`.

[35] B. Andersson, G. Gustafson and L. Lönnblad, Nucl. Phys. B **339** (1990) 393.

[36] A. Kwiatkowski, H. Spiesberger and H. J. Möhring, Comput. Phys. Commun. **69** (1992) 155.

[37] K. Charchula, G. A. Schuler and H. Spiesberger, Comput. Phys. Commun. **81** (1994) 381,
`http://www.desy.de/~hspiesb/djangoh.html`.

[38] B. Andersson, G. Gustafson, G. Ingelman and T. Sjöstrand, Phys. Rept. **97** (1983) 31.

[39] T. Sjöstrand, Comput. Phys. Commun. **39** (1986) 347;

T. Sjöstrand, Comput. Phys. Commun. **82** (1994) 74;

T. Sjöstrand and M. Bengtsson, Comput. Phys. Commun. **43** (1987) 367;

[40] S. D. Ellis and D. E. Soper, Phys. Rev. D **48** (1993) 3160 [hep-ph/9305266];

S. Catani, Y. L. Dokshitzer, M. H. Seymour and B. R. Webber, Nucl. Phys. B **406** (1993) 187.

[41] T. Schörner-Sadenius, Dissertation, University of Munich (2001), Max-Planck-Institut für Physik, München, MPI-PhE/2001-10, (available from `http://www-h1.desy.de/publications/theses_list.html`).

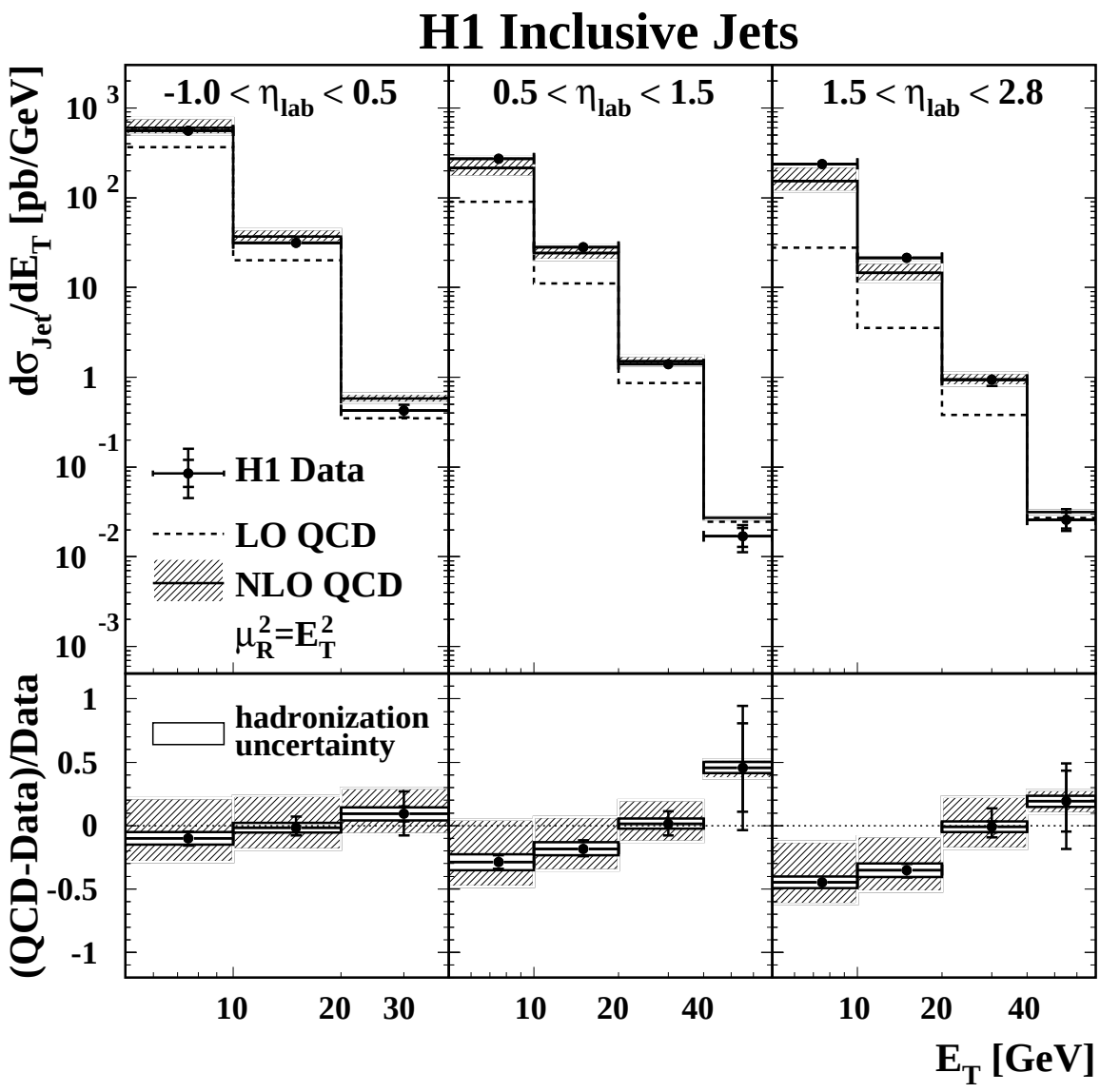

Figure 1: Inclusive jet cross-sections $\mathrm{d}\sigma_{\mathrm{Jet}}/\mathrm{d}E_T$ in different ranges of η_{lab}, integrated over the region $5 < Q^2 < 100$ GeV^2 and $0.2 < y < 0.6$. The data are shown as points with error bars which include statistical and systematic errors. In the top part the data are compared to DISENT NLO QCD calculations using the CTEQ5M parton distribution functions (solid line) and to DISENT LO calculations using CTEQ5L (dashed line). The renormalization scale is set to $\mu_R = E_T$ and no hadronization corrections are applied to these predictions. The hatched band around the NLO prediction stems from variations of the renormalization scale by factors of ± 2. In the bottom part the ratio (QCD-Data)/Data is shown. Here "QCD" denotes NLO QCD corrected for hadronization effects. The inner white band shows the hadronization uncertainty. The hatched outer area contains in addition the renormalization scale uncertainty added linearly. A dotted line at 0 serves to guide the eye.

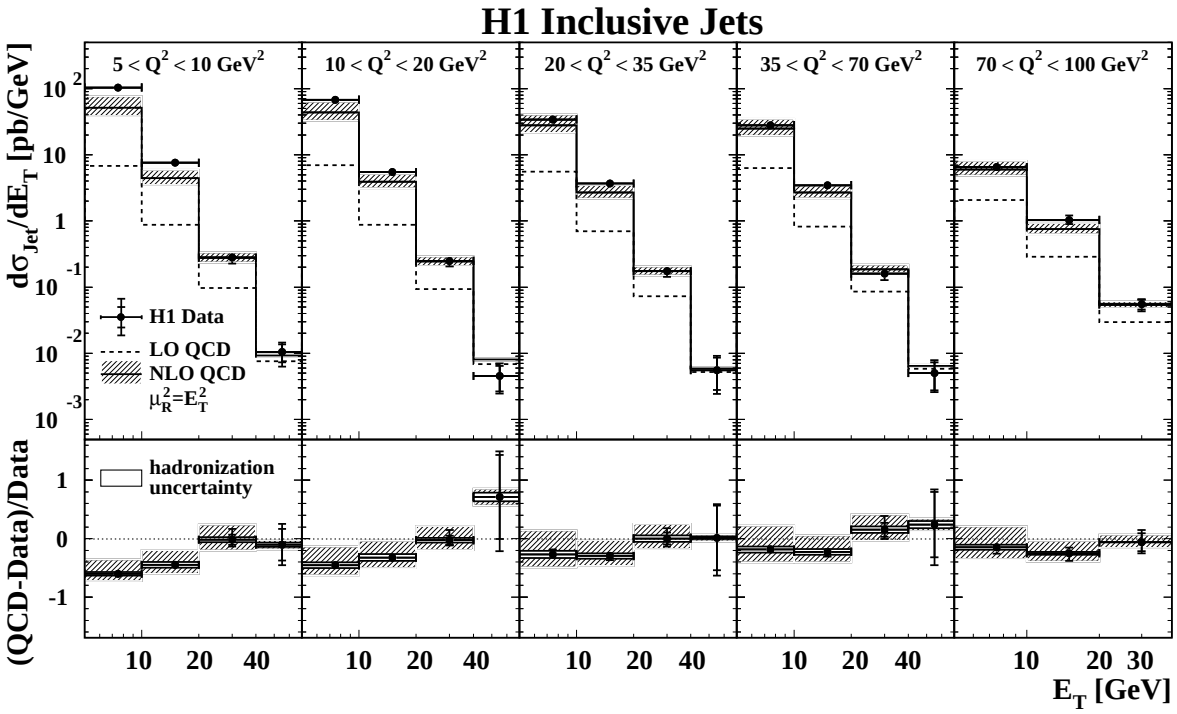

Figure 2: Inclusive jet cross-sections $\mathrm{d}\sigma_{\mathrm{Jet}}/\mathrm{d}E_T$ for the forward region $1.5 < \eta_{\mathrm{lab}} < 2.8$ in different ranges of Q^2. See the caption of figure 1 for further explanation.

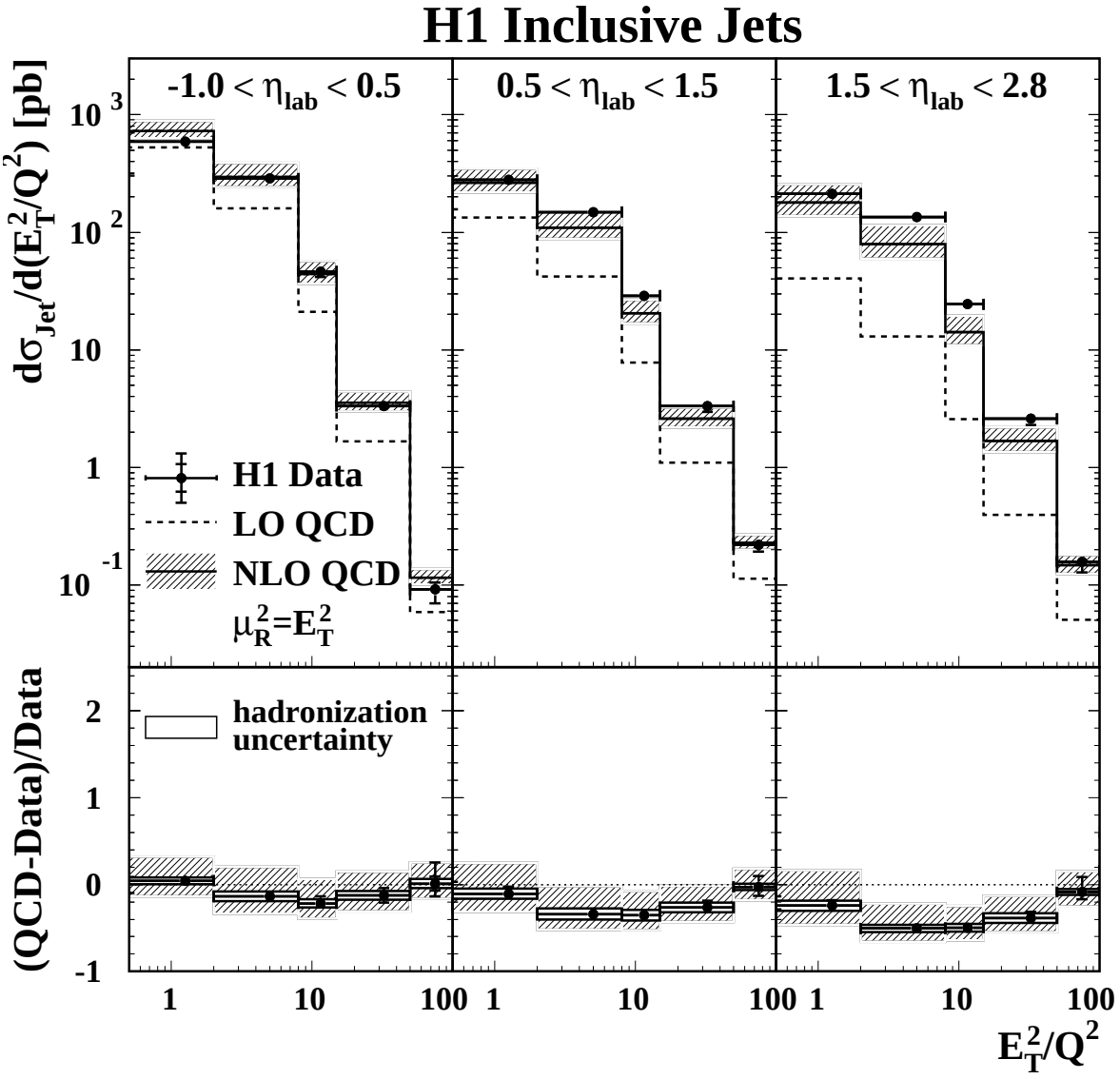

Figure 3: Inclusive jet cross-sections $\mathrm{d}\sigma_{\mathrm{Jet}}/\mathrm{d}(E_T^2/Q^2)$ in different ranges of η_{lab}. See the caption of figure 1 for further explanation.

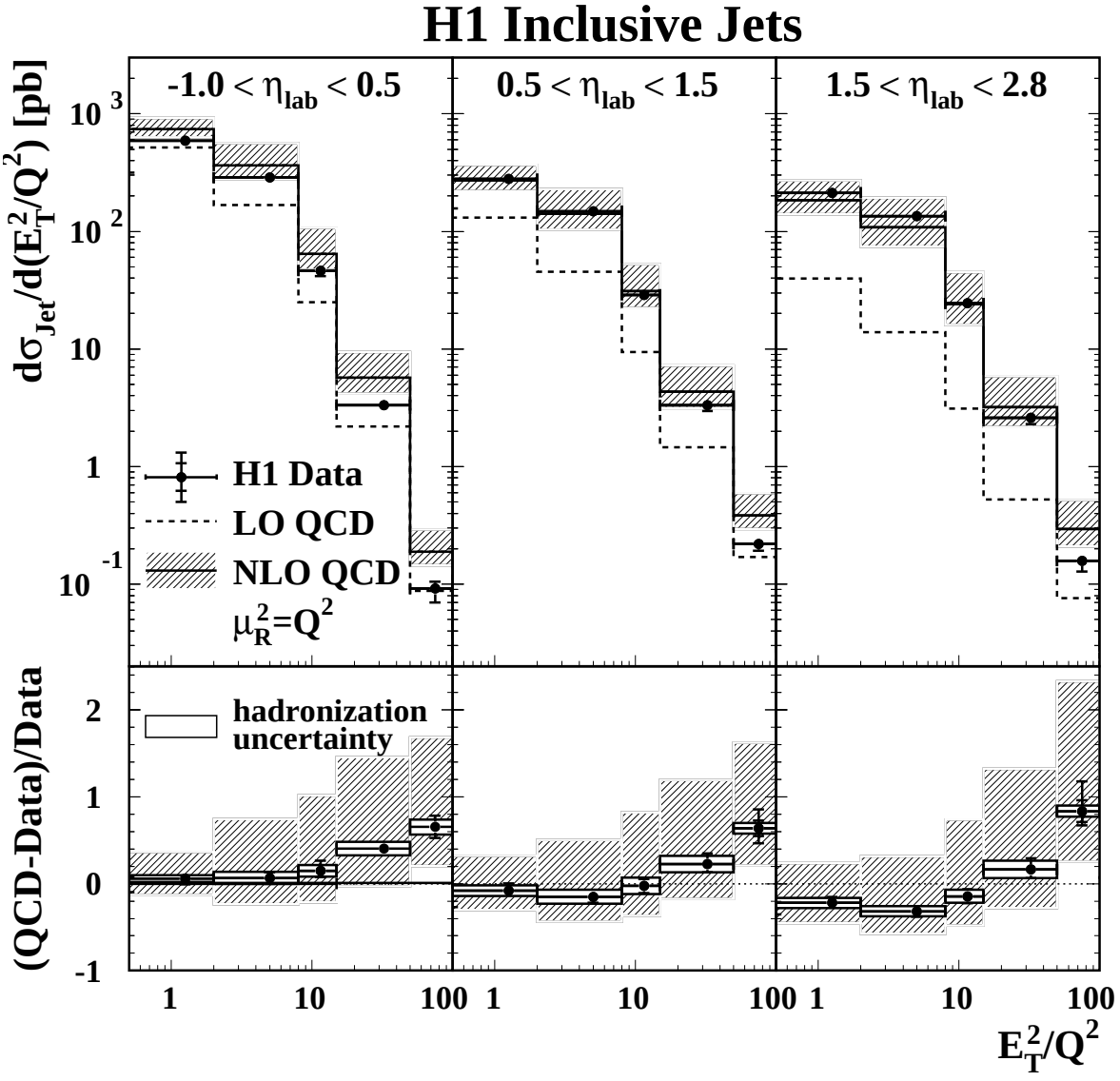

Figure 4: Inclusive jet cross-sections $\mathrm{d}\sigma_{\mathrm{Jet}}/\mathrm{d}(E_T^2/Q^2)$ in different ranges of η_{lab}. Here, the renormalization scale $\mu_R = \sqrt{Q^2}$ is used. See the caption of figure 1 for further explanation.

$\mathrm{d}\sigma_{\mathrm{Jet}}/\mathrm{d}E_T$						
η_{lab} range	E_T interval [GeV]	value [pb/GeV]	stat. error [pb/GeV]	syst. error [pb/GeV]	$< x >$ $[10^{-3}]$	$< Q^2 >$ $[\mathrm{GeV}^2]$
-1.0 - 0.5	5 - 10	561	4	+33 / -35	0.7	21
	10 - 20	31.3	0.5	+2.7 / -2.0		
	20 - 40	0.43	0.03	+0.06 / -0.06		
0.5 - 1.5	5 - 10	272	3	+21 / -19	0.8	23
	10 - 20	28.2	0.5	+2.3 / -2.1		
	20 - 40	1.40	0.07	+0.12 / -0.13		
	40 - 70	0.017	0.006	+0.004 / -0.004		
1.5 - 2.8	5 - 10	238	3	+18 / -18	0.8	21
	10 - 20	21.4	0.5	+1.6 / -1.9		
	20 - 40	0.94	0.06	+0.07 / -0.13		
	40 - 70	0.026	0.008	+0.004 / -0.006		

Table 1: Measured jet cross-sections $\mathrm{d}\sigma_{\mathrm{Jet}}/\mathrm{d}E_T$ in different ranges of η_{lab} for $5 < Q^2 < 100\ \mathrm{GeV}^2$ and $0.2 < y < 0.6$, together with their statistical and systematic uncertainties. The mean values of Bjorken-x and Q^2 of the accepted events are also given.

$d\sigma_{\rm Jet}/dE_T$ for $1.5 < \eta_{\rm lab} < 2.8$						
Q^2 range [GeV^2]	E_T interval [GeV]	value [pb/GeV]	stat. error [pb/GeV]	syst. error [pb/GeV]	$< x >$ [10^{-3}]	$< Q^2 >$ [GeV^2]
5 - 10	5 - 10	104	3	+9 / -11	0.2	7
	10 - 20	7.6	0.4	+0.6 / -0.6		
	20 - 40	0.28	0.03	+0.05 / -0.02		
	40 - 70	0.010	0.005	+0.003 / -0.002		
10 - 20	5 - 10	68.1	1.6	+4.5 / -6.0	0.5	14
	10 - 20	5.5	0.2	+0.4 / -0.4		
	20 - 40	0.25	0.03	+0.04 / -0.01		
	40 - 70	0.005	0.003	+0.001 / -0.002		
20 - 35	5 - 10	34.3	1.4	+4.1 / -1.6	0.9	26
	10 - 20	3.7	0.2	+0.3 / -0.4		
	20 - 40	0.17	0.03	+0.03 / -0.02		
	40 - 70	0.01	0.005	+0.001 / -0.002		
35 - 70	5 - 10	28.0	0.8	+1.9 / -2.1	1.7	49
	10 - 20	3.5	0.2	+0.2 / -0.4		
	20 - 40	0.16	0.02	+0.03 / -0.01		
	40 - 70	0.005	0.005	+0.001 / -0.002		
70 - 100	5 - 10	6.5	0.4	+0.5 / -0.8	3.4	82
	10 - 20	1.03	0.08	+0.12 / -0.06		
	20 - 40	0.055	0.015	+0.008 / -0.006		

Table 2: Measured jet cross-sections $d\sigma_{\rm Jet}/dE_T$ for $0.2 < y < 0.6$ in different ranges of Q^2 for jets in the forward region $1.5 < \eta_{\rm lab} < 2.8$, together with their statistical and systematic uncertainties. The mean values of Bjorken-x and Q^2 of the accepted events are also given.

$d\sigma_{Jet}/d(E_T^2/Q^2)$						
η_{lab} range	E_T^2/Q^2 interval	value [pb]	stat. error [pb]	syst. error [pb]	$< x >$ $[10^{-3}]$	$< Q^2 >$ $[GeV^2]$
-1.0 - 0.5	0.5 - 2	593	6	+32 / -35	1.2	37
	2 - 8	286	3	+17 / -18	0.4	14
	8 - 15	46.3	0.9	+4.7 / -2.7	0.3	9
	15 - 50	3.3	0.1	+0.3 / -0.3	0.2	8
	50 - 100	0.09	0.01	+0.02 / -0.01	0.2	7
0.5 - 1.5	0.5 - 2	280	4	+25 / -15	1.4	39
	2 - 8	149	2	+9 / -12	0.5	15
	8 - 15	28.9	0.7	+2.2 / -2.5	0.4	11
	15 - 50	3.3	0.1	+0.3 / -0.2	0.3	11
	50 - 100	0.22	0.02	+0.03 / -0.02	0.3	9
1.5 - 2.8	0.5 - 2	213	5	+18 / -13	1.4	38
	2 - 8	135	2	+10 / -12	0.5	14
	8 - 15	24.5	0.8	+2.2 / -2.2	0.3	10
	15 - 50	2.6	0.1	+0.3 / -0.2	0.3	9
	50 - 100	0.16	0.02	+0.03 / -0.01	0.3	9

Table 3: Measured jet cross-sections $d\sigma_{Jet}/d(E_T^2/Q^2)$ in different ranges of η_{lab} for $5 < Q^2 < 100\ GeV^2$ and $0.2 < y < 0.6$, together with their statistical and systematic uncertainties. The mean values of Bjorken-x and Q^2 of the accepted events are also given.